IET Generation, Transmission & Distribution

Research Article

IET Journals
The Institution of Engineering and Technology

Adaptive algorithm for estimating power frequency phasors using dynamic window length

ISSN 1751-8687
Received on 13th October 2015
Revised on 24th May 2016
Accepted on 8th June 2016
doi: 10.1049/iet-gtd.2015.1241
www.ietdl.org

Liming Yang, Zaibin Jiao ✉, Xiaoning Kang, Guobing Song, Jiale Suonan

Department of Electrical Engineering, Xi'an Jiaotong University, Xi'an 710049, People's Republic of China
✉ *E-mail: jiaozaibin@mail.xjtu.edu.cn*

Abstract: Estimating phasors as quickly as possible while guaranteeing accuracy is important to ensure reliable fault detection and isolation in power systems. Window length is an important factor for phasor estimation. The conventional fixed window length cannot handle well the many and diverse fault voltage and current signals. By analysing the relationship between accuracy and window length of a phasor estimation using the matrix pencil method, a criterion is established to determine whether or not the estimated phasor is credible. Then, an adaptive algorithm to estimate the phasors using dynamic window length is proposed. Analytical and experimental investigations show that the proposed algorithm can accurately and timely estimate phasors and can enable reliable and quick relay operation.

1 Introduction

Phasor estimation is vital in digital relays [1–4]. Rapidly and accurately estimating the phasor for digital relays is important to reliably detect and isolate faults. In modern power systems, the operating conditions and fault types are different; therefore, the corresponding fault voltage and current signals are diverse. As a result, rapidly and accurately estimating the phasor during fault transient is very difficult. Generally, a more complicated signal demands a longer data window to achieve a sufficiently accurate phasor [5, 6], whereas a longer data window is not necessary in some simple signals. Studying an adaptive algorithm that considers signal complexity is important to estimate the phasor as quickly as possible while ensuring accuracy.

Much research has been carried out on phasor estimation, such as Fourier transform [7–12], recursive-least-squares technique [13], and Newton's method [14]. Fourier algorithm and its improvements have been widely used in phasor estimation owing to their computational efficiency [7–9]. However, because the Fourier algorithm is essentially a decomposition based on a set of sinusoidal signals, it is not suitable for signals that contain inter-harmonic, decaying DC and damped sinusoidal components. The Prony algorithm, which models a signal as a linear combination of exponentials, much better imitates transient signals under fault conditions. The Prony-based algorithms can be more efficient in estimating phasors [15–18]. Hence, an increasing number of Prony-based algorithms, generally categorised as the Prony method and matrix pencil method (MPM), have been profoundly studied in recent years [19, 20]. The efficiency and speed of the MPM-based phasor estimation method have also been dramatically improved [21, 22]. Some researchers have introduced modified MPM to the power system frequency response identifications [23, 24]. However, the performance of these algorithms still cannot satisfy the requirements of relay protection in power systems [25–27].

Although the window length of the Prony-based algorithms can be unrestricted, in practice, the estimation errors of the phasor will be affected by the window length. As we know, speed and accuracy cannot be both simultaneously satisfied in phasor estimation, and they may contradict each other under various conditions. A fixed shorter window will result in an unacceptable estimation error in some complicated fault transients. On the other hand, a fixed longer window is not necessary for some simple fault transients, which may result in additional delay in the tripping process.

This paper presents an adaptive algorithm for estimating phasors using a dynamic window length. By analysing the complexity of a given signal and the rank of the constructed matrix, a criterion is established to determine whether or not the estimated phasor is credible. With the aid of the criterion, when a given signal is simple, a short data window can be selected to quickly estimate the phasor. In contrast, when the given signal is complicated, a longer data window is used to achieve accurate result. The proposed adaptive algorithm can correctly estimate the phasor.

The rest of this paper is organised as follows. Section 2 briefly introduces the phasor estimation algorithm based on MPM and analyses the relationship between the complexity of the signal and the rank of the constructed matrix. Section 3 proposes an adaptive algorithm via a developed criterion. Section 4 shows improvement of the method to deal with a noisy signal. Section 5 verifies the algorithm performance and discusses the effect on the power system protection. Finally, Section 6 presents the conclusion.

2 Basic theory

A phasor estimation algorithm can be designed based on the fundamental MPM theory [22]. The relationship between the window length and accuracy of the estimated phasor is theoretically analysed in the following sections.

2.1 Phasor estimation

We consider a given signal combined by a series of base signals

$$y(n) = \sum_{k=1}^{M} R_{yk} z_k^n = \sum_{k=1}^{M} A_{yk} \exp\left[(\alpha_k + \mathrm{j}2\pi f_k) n T_\mathrm{s} + \mathrm{j}\theta_{yk}\right]. \quad (1)$$

The complex-valued amplitude $R_{yk} = A_{yk} \exp(\mathrm{j}\theta_{yk})$ represents amplitude A_{yk} and initial phase θ_{yk}. Meanwhile, the complex-valued frequency $z_k = \exp[(\alpha_k + \mathrm{j}2\pi f_k)T_\mathrm{s}]$ represents frequency f_k and attenuation factor α_k. M is the number of base signals.

$y(n)$ in (1) is a signal combined by a series of base signals. The base signals $R_k z_k^n$ are complex, but a real signal can be expressed by the combination of these complex signals. From Euler's

formula $\exp(\mathrm{j}\varphi) = cos(\varphi) + \mathrm{j}\sin(\varphi)$, which can be transformed to

$$cos(\varphi) = \frac{\exp(\mathrm{j}\varphi) + \exp(-\mathrm{j}\varphi)}{2} \quad \text{and}$$
$$\sin(\varphi) = \frac{\exp(\mathrm{j}\varphi) - \exp(-\mathrm{j}\varphi)}{2\mathrm{j}},$$

a damped or steady sinusoidal real signal can be expressed as a pair of conjugate complex exponential signals. In addition, a damped or steady offset real signal can easily be expressed as long as f_k is equal to 0. Thus, (1) can describe various electrical signals under transient conditions.

A Hankel matrix can be constructed using the signal

$$\boldsymbol{Y} = \begin{bmatrix} y(0) & y(1) & \cdots & y(L-1) \\ y(1) & y(2) & \cdots & y(L) \\ \vdots & \vdots & \ddots & \vdots \\ y(N-L) & y(N-L+1) & \dots & y(N-1) \end{bmatrix}, \tag{2}$$

where L is the column number of $\boldsymbol{Y}$ and N is the window length for signal processing. L should be chosen in a proper range, i.e.

$$M \le L \le N - M. \tag{3}$$

We choose a unitary reference signal

$$x(n) = z_1^n = \exp(\mathrm{j}2\pi f_1 T_s n). \tag{4}$$

We can prove that the power frequency complex-valued amplitude R_{y1}, i.e. the phasor, of $y(n)$ can be expressed as [22]

$$1/R_{y1} = \boldsymbol{x}_{R1}\boldsymbol{Y}^{+}\boldsymbol{x}_{C1} \tag{5}$$

where $\boldsymbol{Y}^{+}$ is the pseudo-inverse of matrix $\boldsymbol{Y}$ and vectors $\boldsymbol{x}_{R1}$ and $\boldsymbol{x}_{C1}$ are the row and column vectors, respectively, sequentially arranged by $x(n)$.

2.2 Ranks of the matrix and signal

In practice, the result of (5) is accurate when N is sufficiently long; deviation or error will occur if a shorter N is chosen, which can be explained as follows:

Substituting (1) into (2), we obtain

$$\boldsymbol{Y} = \begin{bmatrix} \sum_{k=1}^{M} R_{yk} z_k^0 & \sum_{k=1}^{M} R_{yk} z_k^1 & \cdots & \sum_{k=1}^{M} R_{yk} z_k^{L-1} \\ \sum_{k=1}^{M} R_{yk} z_k^1 & \sum_{k=1}^{M} R_{yk} z_k^2 & \cdots & \sum_{k=1}^{M} R_{yk} z_k^{L} \\ \vdots & \vdots & \ddots & \vdots \\ \sum_{k=1}^{M} R_{yk} z_k^{N-L} & \sum_{k=1}^{M} R_{yk} z_k^{N-L+1} & \dots & \sum_{k=1}^{M} R_{yk} z_k^{N-1} \end{bmatrix}. \tag{6}$$

Equation (6) can be decomposed as

$$\boldsymbol{Y} = \boldsymbol{Z}_A \boldsymbol{R}_y \boldsymbol{Z}_B, \tag{7}$$

where

$$\boldsymbol{Z}_A = \begin{bmatrix} 1 & 1 & \cdots & 1 \\ z_1 & z_2 & \cdots & z_M \\ \vdots & \vdots & \ddots & \vdots \\ z_1^{N-L} & z_2^{N-L} & \cdots & z_M^{N-L} \end{bmatrix}, \tag{8}$$

$$\boldsymbol{Z}_B = \begin{bmatrix} 1 & z_1 & \cdots & z_1^{L-1} \\ 1 & z_2 & \cdots & z_2^{L-1} \\ \vdots & \vdots & \ddots & \vdots \\ 1 & z_M & \cdots & z_M^{L-1} \end{bmatrix}, \tag{9}$$

$$\boldsymbol{R}_y = \mathrm{diag}(R_{y1}, R_{y2}, \dots, R_{yM}). \tag{10}$$

This result can be observed by substituting (8)–(10) into (7), which directly yields (6).

$\boldsymbol{Z}_A$ and $\boldsymbol{Z}_B$ are Vandermonde matrices; thus, they are full-column rank and full-row rank matrices, and both ranks of $\boldsymbol{Z}_A$ and $\boldsymbol{Z}_B$ are M. $\boldsymbol{R}_y$ is a diagonal matrix, and the rank of $\boldsymbol{R}_y$ is M. According to (7), the rank of $\boldsymbol{Y}$ is also M.

For convenience, we define the rank of a signal. If a signal is a linear combination of M damped exponential components such as $y(n)$ in (1), the rank of the signal is defined as M.

Therefore, the rank of $\boldsymbol{Y}$ is equal to the rank of $y(n)$ under normal circumstances.

If signal $y(n)$ is complex, M is large, and N is short, then (3) will not be satisfied, i.e. column L will be less than M, or row $N-L+1$ will be greater than M. Matrix decomposition in (7) cannot be performed. Thus, the fundamental of MPM will be irrational, and the result of (5) will be wrong. In addition, the row or column will be less than M, and the rank of $\boldsymbol{Y}$ will be less than M.

Further, if approximately equal complex-valued frequencies exist, (e.g. z_i) and is close to z_j, distinguishing them in the numerical calculation becomes difficult. Hence, the rank of $\boldsymbol{Y}$ calculated by a practical device will be less than M, and large errors in (5) will occur.

In summary, if

$$\mathrm{rank}(\boldsymbol{Y}) = \mathrm{rank}(y(n)), \tag{11}$$

the result of (5) will be accurate; otherwise, deviation or error will occur.

If the window length of $y(n)$ is sufficiently long, the phasor estimated by (5) can be correct because a sufficiently large matrix $\boldsymbol{Y}$ can be constructed, and the rank of $\boldsymbol{Y}$ can reach M.

3 Adaptive algorithm for phasor estimation

By taking into account the requirement of reliability and speed for power system protection, this section presents an adaptive algorithm for estimating phasors using a dynamic window length.

Voltage and current signals are complicated and many. A criterion is required to determine whether or not the phasor estimated by (5) is credible. With the aid of the criterion, the relay can be properly tripped as quickly as possible.

A straightforward idea is to calculate and compare the ranks of $\boldsymbol{Y}$ and $y(n)$. Unfortunately, in a practical voltage or current signal, the rank of the signal cannot be obtained in advance. Therefore, we cannot directly compare the ranks of the signal and matrix.

The feature of the rank of $\boldsymbol{Y}$ should be determined. When the window length of signal $y(n)$ is long and the size of $\boldsymbol{Y}$ is large, $\boldsymbol{Y}$ will contain much redundant information, and $\boldsymbol{Y}$ can easily express all information of the signal. If two base signals are subtracted from $y(n)$, the rank of $y(n)$ becomes $M-2$, and the rank of $\boldsymbol{Y}$ correspondingly becomes $M-2$.

For instance, if we subtract a power frequency signal from $y(n)$, the ranks of the matrix and the signal become $M-2$. (According

to Euler's formula

$$cos(\varphi) = \frac{\exp(j\varphi) + \exp(-j\varphi)}{2},$$

the power frequency signal corresponds to two base signals.)

If the window length of $y(n)$ is sufficiently short and the size of $\boldsymbol{Y}$ is small, the rank of $\boldsymbol{Y}$ will be less than that of $y(n)$, and $\boldsymbol{Y}$ cannot express all the information of the signal, i.e. the rank of $\boldsymbol{Y}$ is not determined by the number of base signals in $y(n)$ but by the size of $\boldsymbol{Y}$. If two base signals are subtracted from $y(n)$, the rank of $y(n)$ becomes $M-2$. However, the size of $\boldsymbol{Y}$ does not change; thus, the rank of $\boldsymbol{Y}$ will not become $M-2$.

This feature can be used to construct the criterion. For any given $y(n)$, we calculate in advance the phasor R_{y1} using (5) and then transform it to power frequency signal $y_1(n)$ in the time domain. We then subtract the power frequency signal from the original signal $y(n)$.

$$y\_(n) = y(n) - y_1(n). \tag{12}$$

Following the structure of $\boldsymbol{Y}$, we construct $\boldsymbol{Y}\_$ using $y\_(n)$ and compare the ranks of $\boldsymbol{Y}$ and $\boldsymbol{Y}\_$. If

$$\text{rank}(\boldsymbol{Y}\_) = \text{rank}(\boldsymbol{Y}) - 2, \tag{13}$$

the window length of $y(n)$ is sufficiently long, and the result of (5) is credible. If

$$\text{rank}(\boldsymbol{Y}\_) = \text{rank}(\boldsymbol{Y}), \tag{14}$$

the window length of $y(n)$ is not sufficiently long, the result of (5) becomes suspect, and a longer window length is required.

Considering the deviation in the numerical calculation, the constraint in (13) can be minimised as

$$\text{rank}(\boldsymbol{Y}\_) < \text{rank}(\boldsymbol{Y}), \tag{15}$$

and the constraint in (14) can be minimised as

$$\text{rank}(\boldsymbol{Y}\_) \geq \text{rank}(\boldsymbol{Y}) \tag{16}$$

Using the criteria in (15) and (16), the phasor estimated by (5) can be checked. A proper window length can be chosen in advance to estimate the accurate phasor as quickly as possible.

4 Dealing with noisy signals

The practical voltage and current signals can be easily polluted by noise, which may come from signal measurement, conversion, or transmission. Noise influences the rank of the matrix; hence, the above algorithm should be modified.

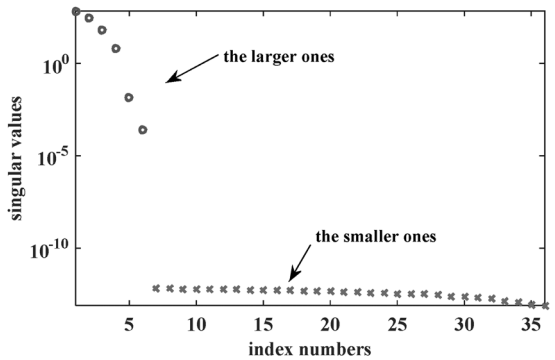

Fig. 1 *Distribution of the singular values of Y*

We consider a given signal with a noise

$$y(n) = \sum_{k=1}^{M} R_{yk} z_k^n + r(n). \tag{17}$$

$y(n)$ is the observed signal, and $r(n)$ is the noisy signal. To reduce the influence of the noisy signal, $y(n)$ can be rewritten as

$$y(n) = \sum_{k=1}^{M} R_{yk} z_k^n + \sum_{k=1}^{rm} R_{yrk} z_{rk}^n + r_1(n). \tag{18}$$

As a finite signal, part of $r(n)$ can be decomposed as $\sum_{k=1}^{rm} R_{yrk} z_{rk}^n$, which has the similar form with the ideal signal, and the rest is represented as $r_1(n)$, which is expected to have smaller influence with ideal signal compared with $r(n)$. The complex-valued amplitude R_{yrk} and complex-valued frequency z_{rk} have similar meaning with R_{yk} and z_k, respectively. rm is the number of base signals of the noise. When rm is large, the approximation in (18) is better. If rm is sufficiently large and the deviation $r_1(n)$ in (18) can be ignored, observed signal $y(n)$ can be constructed as Hankel matrix $\boldsymbol{Y}$ similar to (2). $\boldsymbol{Y}$ can be decomposed as

$$\boldsymbol{Y} = \boldsymbol{Z}_{Ar} \boldsymbol{R}_{yr} \boldsymbol{Z}_{Br} \tag{19}$$

where

$$\boldsymbol{Z}_{Ar} = \begin{bmatrix} 1 & 1 & \cdots & 1 & 1 & \cdots & 1 \\ z_1 & z_2 & \cdots & z_M & z_{r1} & \cdots & z_{rm} \\ \vdots & \vdots & \ddots & \vdots & \vdots & \ddots & \vdots \\ z_1^{N-L} & z_2^{N-L} & \cdots & z_M^{N-L} & z_{r1}^{N-L} & \cdots & z_{rm}^{N-L} \end{bmatrix}, \tag{20}$$

$$\boldsymbol{Z}_{Br} = \begin{bmatrix} 1 & z_1 & \cdots & z_1^{L-1} \\ 1 & z_2 & \cdots & z_2^{L-1} \\ \vdots & \vdots & \ddots & \vdots \\ 1 & z_M & \cdots & z_M^{L-1} \\ 1 & z_{r1} & \cdots & z_{r1}^{L-1} \\ \vdots & \vdots & \ddots & \vdots \\ 1 & z_{rm} & \cdots & z_{rm}^{L-1} \end{bmatrix}, \tag{21}$$

$$\boldsymbol{R}_{yr} = \text{diag}(R_{y1}, R_{y2}, \ldots, R_{yM}, R_{yr1}, \ldots, R_{yrm}). \tag{22}$$

Our study is concerned with the ideal components of $y(n)$; therefore, the definition of the rank of the observed signal is still M, which is the number of ideal base signals.

For consistency with Section 3, the rank of matrix $\boldsymbol{Y}$ should be redefined. The rank of $\boldsymbol{Y}$ should only reflect the ideal part of the signal.

We consider the singular values of $\boldsymbol{Y}$. The typical singular value distribution is shown in Fig. 1.

Fig. 1 shows that the singular values can be divided into two categories. Some of them are much larger than the others. The large ones represent the ideal part of the observed signal, whereas the small ones represent the noisy part.

Thus, we redefine the rank of the matrix as the number of large singular values.

Some distributions of the singular values are not easy to distinguish. Some algorithms give a threshold or relative threshold to count the number of large singular values. We set the maximum curvature of the singular values as the threshold, and the rank of the matrix can be determined.

From the redefinition of the rank of a matrix, the criteria expressed in (15) and (16) can also be suitable for signals with noise.

Thus, for any voltage or current signals, whether polluted or not, an adaptive algorithm can be applied to estimate phasors using a dynamic window length.

Table 1 Phasor estimation for $y_1(n)$

Window length, ms	Rank (Y)	Rank ($Y\_$)	Credible	Amplitude	Phase (°)	TVE, %
1	4	4	×	10.67	42.90	7.70
2	6	5	√	10.00	45.00	0.00

5 Performance evaluation

Phasors of various ideal or noisy signals are estimated to ensure the validity of the proposed algorithm. The effect on power system protection is investigated. Comparison of the proposed and conventional algorithms is also presented.

5.1 Performance verification

In this section, the window length is chosen using the criteria in (15) and (16) for the constructed signals, and phasors are estimated to verify the performance of the proposed algorithm.

The sampling rate of the constructed signal is 10 kHz. In the following section, the window length is measured by time (ms). It is another representation of window length N. As $N = T \cdot f_s$, 1 ms is equivalent to 10 sampling values. The parameter L, which is used in the process of the proposed algorithm, is empirically set as an integer which is around $N/3$.

5.1.1 Verification of ideal constructed signals: We consider the signal with harmonic components

$$y_1(n) = 10\sin(\omega_1 t + \pi/4) + \sin(2\omega_1 t) + 2\sin(3\omega_1 t + \pi/6), \quad (23)$$

where $\omega_1 = 2\pi f_1$ and $f_1 = 50$ Hz. We estimate the phasor using the proposed algorithm.

The window length used for the estimation, the ranks of $\boldsymbol{Y}$ and $\boldsymbol{Y}\_$, the determination whether the result is credible or not, the amplitude, and the initial phase of the phasor are listed in Table 1. The total vector error (TVE) is also introduced to show errors of phasor estimation. TVE is defined as

$$\mathrm{TVE} = \sqrt{\frac{(X_\mathrm{r} - X_{0\mathrm{r}})^2 + (X_\mathrm{i} - X_\mathrm{i})^2}{X_{0\mathrm{r}}^2 + X_{0\mathrm{i}}^2}},$$

where X_r and X_i are, respectively, the real and imaginary parts of estimates given by the proposed algorithm, and $X_{0\mathrm{r}}$ and $X_{0\mathrm{i}}$ are the corresponding parts of theoretical values. The correct amplitude and initial phase should be 10 and 45, respectively.

If we use 1 ms as the window length, the ranks of $\boldsymbol{Y}$ and $\boldsymbol{Y}\_$ are equal. According to the criterion in (16), the estimated phasor is not credible. The calculated amplitude and initial phase are shown in columns 5 and 6, respectively. They show large deviations, and the criterion in (16) is available. This result indicates that a longer window should be applied to obtain more accurate results.

If we use 2 ms as the window length, the rank of $\boldsymbol{Y}\_$ is less than that of $\boldsymbol{Y}$. According to the criterion in (15), the estimated phasor is credible. The calculated amplitude and initial phase are shown in columns 5 and 6, respectively. We can see that they are accurate, and the criterion in (15) is available.

Table 2 Phasor estimation for $y_2(n)$

Window length, ms	Rank (Y)	Rank ($Y\_$)	Credible	Amplitude	Phase (°)	TVE, %
2	6	6	×	11.89	50.73	21.82
5	7	7	×	9.98	45.01	0.20
10	9	8	√	10.00	45.01	0.02

Table 3 Phasor estimation for $y_3(n)$

Window length, ms	Rank (Y)	Rank ($Y\_$)	Credible	Amplitude	Phase (°)	TVE, %
1	3	2	√	10.00	45.00	0.00

The signal is constructed, so the rank of $y_1(n)$ can be acquired previously. As $y_1(n)$ is combined by 3 sinusoidal signals, the rank of $y_1(n)$, M, is 6. As can be seen, the rank of $\boldsymbol{Y}$ is equal to the rank of $y_1(n)$ when we use 2 ms as the window length; they are not equal when we use 2 ms as the window length. This conforms to our theoretical analysis.

The signal in (23) is simple; thus, we can easily and accurately estimate the phasor using a very short window length. Tripping the relay without superfluous delay is certainly helpful.

Let us consider a more complicated signal,

$$y_2(n) = 10\sin(\omega_1 t + \pi/4) + \sin(2\omega_1 t) + 2\sin(3\omega_1 t + \pi/6) + 3\exp(-0.01t) + 2\sin(2\omega_1 t)\exp(-20t), \quad (24)$$

which contains harmonics, decaying DC, and damped sinusoidal components. We estimate the phasor using the proposed algorithm.

Different window lengths are chosen to estimate the phasor. As listed in Table 2, when the window length is set to 2 or 5 ms, the ranks of $\boldsymbol{Y}$ and $\boldsymbol{Y}\_$ satisfy the conditions in (16) and indicate that the estimated phasor are not credible. The calculated amplitude and initial phase shown in columns 5 and 6, respectively, verify the decision. A longer window length of 10 ms is applied, and the rank of $\boldsymbol{Y}\_$ is less than that of $\boldsymbol{Y}$. Thus, the calculated amplitude and initial phase shown in columns 5 and 6, respectively, are credible.

As the decaying DC component is corresponding to one base signal and the other three components are corresponding to two base signals, respectively, the rank of $y_2(n)$, M, is 9. This agrees with the results.

The signal in (24) is more complicated than that in (23); thus, more information, i.e. longer window length, is required to obtain a credible phasor. In some conditions, the voltage or current signals after a system fault are messy. Delaying the relay waiting time for correct phasor is thus necessary.

As the proposed algorithm is based on a signal which is combined by series of complex-valued signals, it is naturally applicable for complex-valued signals. Without loss of generality, consider the following signal,

$$y_3(n) = 10\exp(\mathrm{j}\omega_1 t + \mathrm{j}\pi/4) + \exp(\mathrm{j}2\omega_1 t) + 2\exp(\mathrm{j}3\omega_1 t + \mathrm{j}\pi/6), \quad (25)$$

where $\omega_1 = 2\pi f_1$ and $f_1 = 50$ Hz. We estimate the phasor using the proposed algorithm (Table 3).

The result is similar with the real signals. It is worth noting that $\boldsymbol{Y}\_$ is also constructed by a complex-valued signal. The amplitude, and the initial phase of the phasor are estimated correctly.

5.1.2 Verification of constructed signals with noise: The voltage or current signals acquired in practice will inevitably be polluted by noise. We add a white Gaussian noise in which the

Table 4 Phasor estimation for $y_1(n)$ with noise

Window length ms	Rank (Y)	Rank ($Y\_$)	Credible	Amplitude	Phase (°)	TVE, %
10	5	6	×	11.36	39.38	17.15
15	6	5	√	10.00	44.99	0.02

Table 5 Phasor estimation for $y_2(n)$ with noise

Window length, ms	Rank (Y)	Rank ($Y\_$)	Credible	Amplitude	Phase (°)	TVE, %
15	7	7	×	9.62	47.27	5.44
30	9	8	√	10.00	44.99	0.02

signal-to-noise ratio is 50 dB to the ideal signals in (23) and (24). We estimate the phasor using the proposed algorithm.

The phasor estimation for $y_1(n)$ with noise is listed in Table 4. According to the criteria in (15) and (16), a 15-ms window length is required to obtain a credible result.

The phasor estimation for $y_2(n)$ with noise is listed in Table 5. According to the criteria in (15) and (16), a 30-ms window length is required to obtain a credible result.

Signals polluted by noise are more complicated than ideal signals. As expressed in (18), to simulate as much as possible the noisy components of the signal using base signals, a large *rm*, which is the number of base signals, may be required. Thus, a long window should be used to estimate the phasor.

5.2 Response time

The aim of the proposed algorithm is to estimate the phasor as quickly as possible while guaranteeing accuracy. Hence, the response time of the proposed algorithm should be investigated. The response time is dependent on the asymptotic time complexity and the window length.

The asymptotic time complexity can represent the computational burden for practical application. As addition is much easier than multiplication, the asymptotic time complexity is approximately the count of multiplications used in an algorithm. The asymptotic time complexity of the proposed algorithm is $O(N^3)$. It is larger than that of Fourier algorithm, which is $O(N)$. It means that for the same window length, the proposed algorithm has to deal with much more multiplications than Fourier algorithm. Hence the data processing time of them will be different in the same hardware equipment. A simple test about time consumption of the proposed and Fourier algorithms has been made and the comparison is shown in Fig. 2.

The relative time consumption of the proposed and Fourier algorithms can be obtained intuitively in Fig. 2. Much more time needed for the data processing of the proposed algorithm. When the computing device is not efficient, this part of response time will be remarkable. However, the time consumption of data processing of an algorithm is not inherent, but related with the performance of hardware. In recent years, the computing speed of signal processing devices has been dramatically improved, especially after using the technology of hardware multiplication. Hence, this part of response time will become smaller and smaller with the development of hardware.

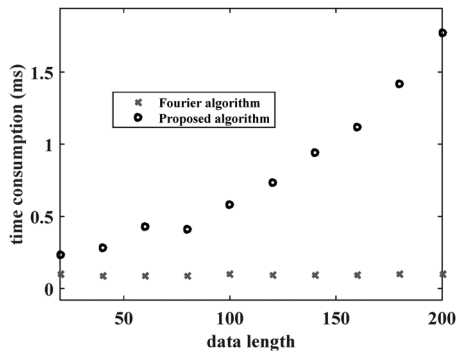

Fig. 2 *Comparison of time consumption of the proposed and Fourier algorithm*

Another part of response time is dependent on the window length. For any phasor estimation algorithm, there must be long enough input sequence to generate the correct output. The window length of Fourier algorithm is usually 20 ms (one cycle, when the power frequency is 50 Hz), and the window length for half-cycle Fourier algorithm is 10 ms. The proposed algorithm has adaptive window length. When the input signal is simple, the window length needed is very short. For example, as shown in Table 1 in Section 5.1, Only 2 ms are needed to estimate a phasor. When the signal is very complicated or severely polluted by noise, a long window length is needed. Generally, the proposed algorithm can quickly give accurate results with acceptable computational burden in most instances, and can also prevent suspect phasor misleading power system protections on rare conditions.

Considering two factors of response time, the asymptotic time complexity and the window length, and the development of field devices, the proposed algorithm has a more competitive prospect.

5.3 Influence of sampling rate

A higher sampling rate will provide more signal information and result in higher accuracy [22]. Under the same period, a higher sampling rate get a longer sampling value range, and the constructed matrix will be larger and easier to conform on (11). That is, under different sampling rate, the proposed algorithm will adaptively choose different window length to estimate phasors. Considering the signal in (23), we test the sampling rates 2.5, 5, and 10 kHz, which are widely used in practice, as well as 500 Hz, and 20 kHz for contrast. The chosen window lengths are shown in Fig. 3.

As illustrated in Fig. 3, higher sampling rates need shorter window length to give accurate results. If the sampling rate is higher than 10 kHz, it has little influence on the chosen window length. Similar results can be obtained with the signal given in (24). In practical application, the sampling rate depends on PTs and CTs deployed in the substations. The proposed algorithm can adapt to kinds of sampling rate.

5.4 Effect on power system protection

Phasors can be quickly and accurately estimated using the proposed algorithm. Thus, protection methods based on phasors can be improved. The performance of the distance protection is evaluated as follows: a double-end power system simulation model was built in PSCAD, and the single-line diagram is shown in Fig. 4.

The system is operated at 50 Hz, and the parameters of the system are listed in Table 6.

The distance protection deployed at the left side of a 100-km transmission line is investigated. The set point for the distance protection is 90% of the entire line. The sampling rate is 10 kHz.

5.4.1 Strategy of window length selecting: The criteria in (15) and (16) just judge the given window length is proper or not.

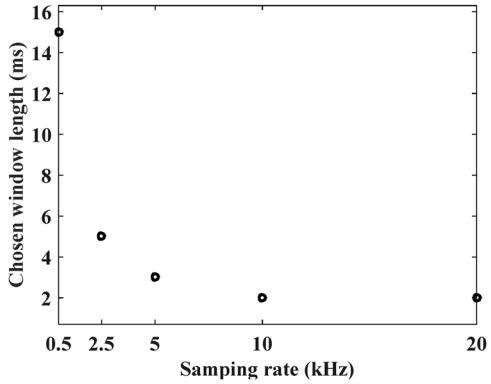

Fig. 3 *Chosen window lengths at different sampling rates*

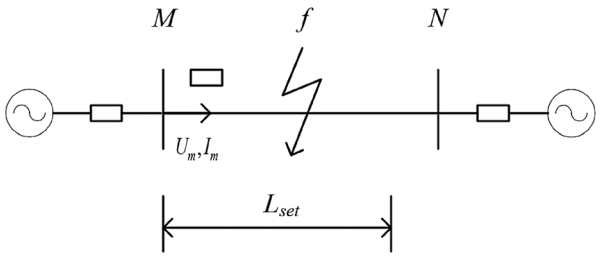

Fig. 4 *Double-end power system simulation model*

For practical application, a strategy to obtain an optimal window length should be given. The intuitive way is to test every window length from the minimum to a proper value step by step. It will cost extremely high computational burden and it is not necessary.

The strategy of window length selecting should be cooperated with its practical scenarios. Different relays have different requirements of time response. For a specific relay, a group of window lengths should be prepared beforehand. If the phasor is provided for fast relays, small window lengths should be tested; if the phasor is used by backup protections or delayed relays, large window lengths should be tested. For instance, if the phasor is used for zone I distance protection, the group of window lengths can be chosen as 5, 10, 15, 20, 25 and 30 ms. Then apply the criteria for the most ordinary window length. If it is feasible, try to reduce the window length until it is not feasible; if it is not feasible, try to enlarge the window length until it is feasible. The flow chart is shown below.

In Fig. 5, T0 is the most ordinary window length, such as 20 ms for zone I distance protection, and dT is the interval of different window length, such as 5 ms. T1 and T2 are auxiliary variables and T is the proper window length. It is worth noting that when the minimum window length is feasible, the proper window length should be the minimum window length; when the maximum window length is not feasible, it should be reported that no proper window length exist. As the group of window length is not large, the proper window length could be decided with at most 4 times' judgment for zone I protection.

5.4.2 Verification of the internal fault: A single-phase (phase A) fault at 80% of the entire line is introduced after 0.3 s. The current and voltage signals are shown in Fig. 6.

Today, phasors used for distance protection are estimated using the Fourier algorithm. The distance protections using the Fourier and proposed algorithms are compared.

The full-cycle Fourier algorithm, i.e. a window length of 20 ms, is used to estimate the phasors of the voltage and current signals. Then, the measured impedance can be obtained by

$$Z_m = \frac{V_{ma}}{I_{ma} + k \cdot 3I_{m0}} \tag{26}$$

where V_{ma} and I_{ma} are the phasor of the voltage and current in phase A, respectively, and I_{m0} is the zero-sequence current. k is the zero-sequence compensation factor, which can be obtained using zero-sequence impedance z_0 and positive impedance z_1 of the transmission line, i.e.

$$k = \frac{z_0 - z_1}{3z_1}. \tag{27}$$

The impedance characteristic seen from bus M is shown in Fig. 7. The operating zone is enlarged and shown at the top right corner.

Fig. 7 shows that the impedance characteristic curve enter the operating zone 18 ms after the fault occurs. Because of the cross-window data, which contain both the normal operating data and fault data, the time when the impedance characteristic curve enters the operating zone is shorter than 20 ms. The relay does not immediately trip at 18 ms but waits for a short period such as Δt to confirm the decision. Thus, the relay will trip at $\Delta t + 18$ ms after the fault.

Subsequently, we evaluate the performance of the distance protection using the phasor estimated by the proposed algorithm. According to the criteria in (15) and (16) and the flow chart in Fig. 2, after 3 times' judgment, the window length is set at 10 ms after the voltage and current signals are tested. Using the same procedure, the impedance characteristic seen from bus M is shown in Fig. 8.

Fig. 8 shows that the impedance characteristic curve enters the operating zone 9.2 ms after the fault occurs. Because of the cross-window data, the time when the impedance characteristic curve enters the operating zone is shorter than 10 ms. Thus, the relay will trip at $\Delta t + 9.2$ ms after the fault.

Because the voltage and current signals shown in Fig. 6 are not very complicated, the phasor estimation can be accurately accomplished in a very short window length. Using the full-cycle Fourier algorithm requires more time delay to trip the relay and may compromise the safety of the power system.

Fig. 9 shows the impedance characteristic seen from bus M if we instead use the half-cycle Fourier algorithm.

Table 6 Parameters of the line and source impedances

Parameters	Value
length of transmission line	100 km
positive-sequence impedance of transmission line	0.018 + j0.262 Ω/km
zero-sequence impedance of transmission line	0.178 + j0.670 Ω/km
positive-sequence source impedance at the left-side	2 + j26.39 Ω
zero-sequence source impedance at the left-side	3 + j75 Ω
positive-sequence source impedance at the right-side	j24.12 Ω
zero-sequence source impedance at the right-side	j69 Ω

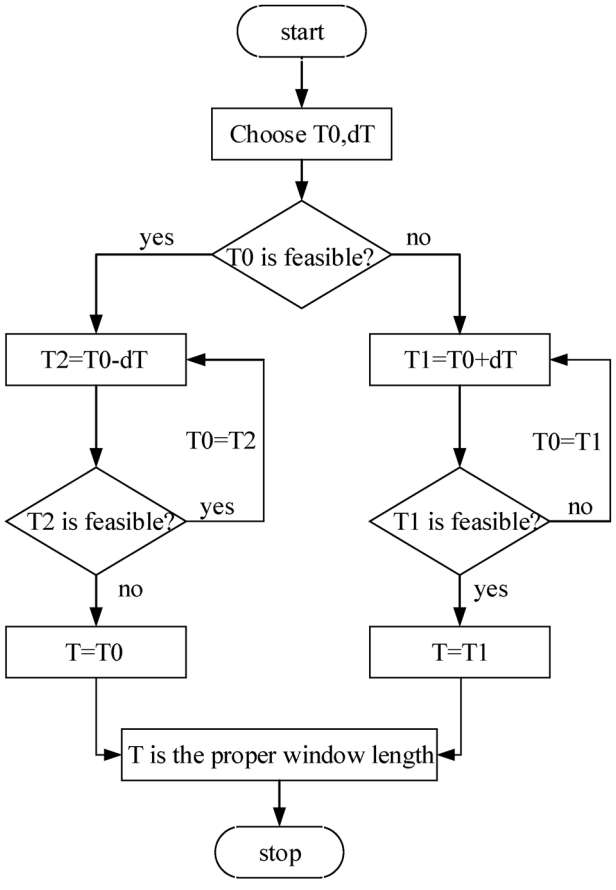

Fig. 5 *Flow chart of strategy of window length selecting*

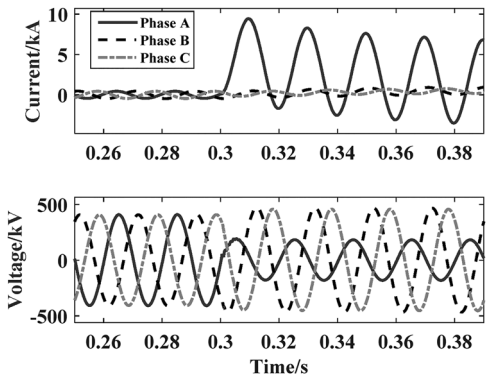

Fig. 6 *Current and voltage signals when a single-phase fault occurs*

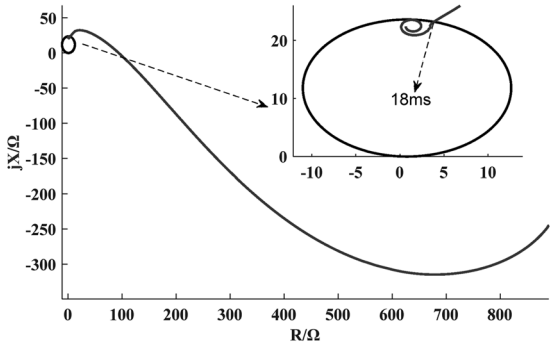

Fig. 7 *Impedance characteristic obtained using the Fourier algorithm*

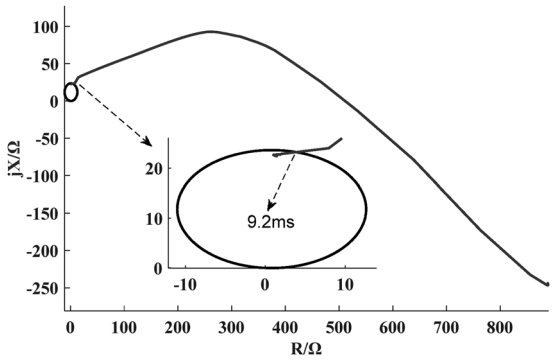

Fig. 8 *Impedance characteristic obtained using the proposed algorithm*

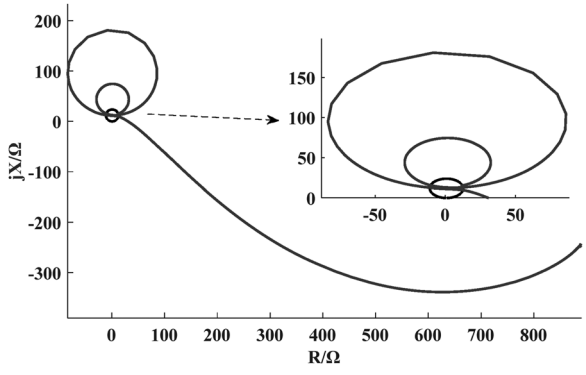

Fig. 9 *Impedance characteristic obtained using the half-cycle Fourier algorithm*

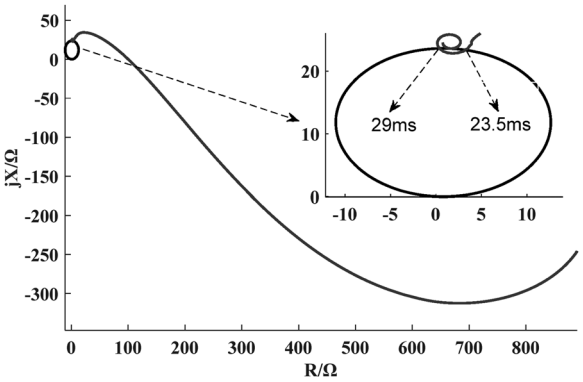

Fig. 10 *Impedance characteristic obtained using the Fourier algorithm*

Fig. 9 shows that the decaying DC components in the voltage and current signals strongly disturb the half-cycle Fourier algorithm, and the estimated phasors are not reliable. The impedance characteristic curve enters and then comes out of the operating zone. Thus, the distance protection cannot decide to trip the relay.

If no criterion is set to verify the estimated phasor, the window length may be set too long and delay the relay tripping or too short to result in erroneous relay operation.

5.4.3 Verification of external fault: A single-phase (phase A) fault at the head end of the next line is set after 0.3 s. The current and voltage signals are shown in Fig. 6. The distance protections using the Fourier and proposed algorithms are also compared.

The full-cycle Fourier algorithm is used to estimate the phasors of the voltage and current signals. The impedance characteristic seen from bus *M* is shown in Fig. 10.

Fig. 10 shows that the impedance characteristic curve enters the operating zone at 23.6 ms and comes out of the operating zone at 29 ms. The relay may erroneously operate during this time. Although the impedance characteristic curve is stable at a point out of the operating zone with a short time delay, the deviations in the estimation of phasors of the voltage and current signals, which result in the deviations in the impedances, may cause erroneous operation of the distance relay.

The performance of the distance protection using the phasor estimated by the proposed algorithm is then investigated. According to the criteria in (15) and (16) and the flow chart in Fig. 2, after 3 times' judgment, the window length is also set to 10 ms. The impedance characteristic seen from bus *M* is shown in Fig. 11.

Fig. 11 shows that the impedance characteristic curve does not enter the operating zone at all times. Because the phasors estimated by the proposed algorithm are accurate and stable, erroneous operation can be avoided.

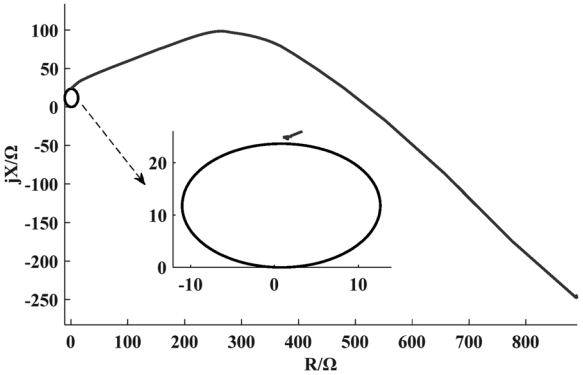

Fig. 11 *Impedance characteristic obtained using the proposed algorithm*

6 Conclusions

An adaptive algorithm for estimating phasors using a dynamic window length has been proposed. According to the analytical and experimental investigations presented in this paper, the following conclusions are drawn:

(i) A criterion is proposed to determine whether the phasor estimated by MPM is credible or not.
(ii) A proper window length can be chosen to estimate the accurate phasor as quickly as possible.
(iii) The proposed algorithm can help in reliable and quick tripping of the relay.

Because phasors are the basis of power system protection, accurate and fast estimation algorithm is expected to be an attractive prospect for their determination.

7 Acknowledgment

This work was supported in part by the National Natural Science Foundation of China (grant no. 51377129).

8 References

1 Coffele, F., Booth, C., Dysko, A.: 'An adaptive overcurrent protection scheme for distribution networks', *IEEE Trans. Power Deliv.*, 2015, **30**, pp. 561–568
2 Das, S., Karnik, N., Santoso, S.: 'Distribution fault-locating algorithms using current only', *IEEE Trans. Power Deliv.*, 2012, **30**, pp. 1144–1153
3 Lin, X., Li, Z., Ke, S., *et al.*: 'Theoretical fundamentals and implementation of novel self-adaptive distance protection resistant to power swings', *IEEE Trans. Power Deliv.*, 2010, **35**, pp. 1372–1383
4 Wang, B., Dong, X., Bo, Z., *et al.*: 'Negative-sequence pilot protection with applications in open-phase transmission lines', *IEEE Trans. Power Deliv.*, 2010, **25**, pp. 1306–1313
5 Phadke, A.G., Thorp, J.S.: 'Computer relaying for power systems' (John Wiley & Sons Ltd., 2009), pp. 16–19, 176–180
6 Horowitz, S.H., Phadke, A.G.: 'Power system relaying' (Research Studies Press Limited, 2008, 3rd edn.), p. 22
7 Abbas, S.A.: 'A new fast algorithm to estimate real-time phasors using adaptive signal processing', *IEEE Trans. Power Deliv.*, 2013, **28**, (2), pp. 807–815
8 Kang, S.H., Lee, D.G., Nam, S.R., *et al.*: 'Fourier transform-based modified phasor estimation method immune to the effect of DC offsets', *IEEE Trans. Power Deliv.*, 2009, **24**, (3), pp. 1104–1111
9 Wei-Hsin, C., Nguyen, T.Q.: 'On the fixed-point accuracy analysis of FFT algorithms', *IEEE Trans. Signal Process.*, 2008, **56**, pp. 4673–4682
10 Zhang, P., Xue, H., Yang, R., *et al.*: 'Shifting window average method for phasor measurement at off-nominal frequencies', *IEEE Trans. Power Deliv.*, 2014, **29**, (3), pp. 1063–1073
11 Zhang, P., Xue, H., Yang, R.: 'Shifting window average method for accurate frequency measurement in power systems', *IEEE Trans. Power Deliv.*, 2011, **26**, (4), pp. 2887–2889
12 Belega, D., Macii, D., Petri, D.: 'Fast synchrophasor estimation by means of frequency-domain and time-domain algorithms', *IEEE Trans. Instrum. Meas.*, 2014, **63**, (2), pp. 338–401
13 Sadinezhad, I., Agelidis, V.G.: 'Real-time power system phasors and harmonics estimation using a new decoupled recursive-least-squares technique for DSP implementation', *IEEE Trans. Ind. Electron.*, 2013, **60**, (6), pp. 2295–2308
14 Dash, P.K., Krishnanand, K.R., Padhee, M.: 'Fast recursive GaussNewton adaptive filter for the estimation of power system frequency and harmonics in a noisy environment', *IET Gener. Transm. Distrib.*, 2011, **5**, (12), pp. 1277–1289
15 Hua, Y., Sarkar, T.K.: 'Matrix pencil method for estimating parameters of exponentially damped/undamped sinusoids in noise', *IEEE Trans. Acoust. Speech Signal Process.*, 1990, **38**, (5), pp. 814–824
16 Hua, Y., Sarkar, T.K.: 'On SVD for estimating generalized eigenvalues of singular matrix pencil in noise', *IEEE Trans. Signal Process.*, 1991, **39**, (4), pp. 892–900
17 Hua, Y.: 'Estimating two-dimensional frequencies by matrix enhancement and matrix pencil', *IEEE Trans. Signal Process.*, 1992, **40**, (9), pp. 2267–2280
18 Sarkar, T.K., Pereira, O.: 'Using the matrix pencil method to estimate the parameters of a sum of complex exponentials', *IEEE Antennas Propag. Mag.*, 1995, **37**, (1), pp. 48–55
19 Catedra, M.F., Rivas, F., Delgado, C., *et al.*: 'Application of matrix pencil to obtain the current modes on electrically large bodies', *IEEE Trans. Antennas Propag.*, 2006, **54**, pp. 2429–2436
20 Peilin, F., Niculescu, S.I., Jie, C.: 'Stability of linear neutral time-delay systems: exact conditions via matrix pencil solutions', *IEEE Trans. Autom. Control*, 2006, **51**, pp. 1063–1069
21 Suonan, J., Wang, B., Wang, L., *et al.*: 'A fast phasor calculation algorithm for power systems'. Proc. 2013 CSEE, pp. 123–129 (in Chinese)
22 Yang, L., Jiao, Z., Kang, X., *et al.*: 'Fast algorithm for estimating power frequency phasors under power system transients', *IET Gener. Transm. Distrib.*, 2015, **9**, pp. 395–403
23 Sheshyekani, K., Karami, H.R., Dehkhoda, P., *et al.*: 'Application of the matrix pencil method to rational fitting of frequency domain responses', *IEEE Trans. Power Deliv.*, 2012, **27**, (4), pp. 2399–2408
24 Sheshyekani, K., Tabei, B.: 'Multiport frequency-dependent network equivalent using a modified matrix pencil method', *IEEE Trans. Power Deliv.*, 2014, **29**, (5), pp. 2340–2348
25 Zhong, Y., Kang, X., Jiao, Z., *et al.*: 'A novel distance protection algorithm for the phase-ground fault', *IEEE Trans. Power Deliv.*, 2014, **29**, pp. 1718–1725
26 Wang, C., Song, G., Kang, X., *et al.*: 'Novel transmission-line pilot protection based on frequency-domain model recognition', *IEEE Trans. Power Deliv.*, 2015, **30**, pp. 1243–1250
27 Wang, H., Song, G., Ding, J., *et al.*: 'Long line distance protection based on fast phasor calculation algorithm'. IET Conf. Publications, 2014 12th IET Int. Conf. on Developments in Power System Protection, DPSP, 2014